Histone H1 is essential for mitotic chromosome architecture and segregation in *Xenopus laevis* egg extracts

Thomas J. Maresca, Benjamin S. Freedman, and Rebecca Heald

Department of Molecular and Cell Biology, University of California, Berkeley, Berkeley, CA 94720

During cell division, condensation and resolution of chromosome arms and the assembly of a functional kinetochore at the centromere of each sister chromatid are essential steps for accurate segregation of the genome by the mitotic spindle, yet the contribution of individual chromatin proteins to these processes is poorly understood. We have investigated the role of embryonic linker histone H1 during mitosis in *Xenopus laevis* egg extracts. Immunodepletion of histone H1 caused the assembly of aberrant elongated chromosomes that extended off the metaphase plate and outside the perimeter of the spindle. Although functional kinetochores assembled, aligned, and exhibited poleward movement, long and tangled chromosome arms could not be segregated in anaphase. Histone H1 depletion did not significantly affect the recruitment of known structural or functional chromosomal components such as condensins or chromokinesins, suggesting that the loss of H1 affects chromosome architecture directly. Thus, our results indicate that linker histone H1 plays an important role in the structure and function of vertebrate chromosomes in mitosis.

Introduction

Correct transmission of the genome by the mitotic spindle during cell division requires dramatic changes in chromosome architecture. Chromosome condensation, which in vertebrates reduces chromosome length ~100–500-fold relative to interphase, is crucial to physically resolve entanglements and allow separation of the duplicated genome into two discrete sets (Heck, 1997). In addition, the assembly of a specialized macromolecular structure called the kinetochore at the centromere of each sister chromatid is necessary to mediate chromosome attachment and movement within the spindle (Cleveland et al., 2003). Failure to properly segregate chromosomes can cause cell death and lead to birth defects or cancer. Despite the fundamental importance of higher order chromosome organization to the faithful segregation of the genome, molecular mechanisms governing mitotic chromosome structure remain poorly understood.

Major factors that are known to impose higher order mitotic chromosome architecture include topoisomerase II (Swedlow and Hirano, 2003) and the multisubunit ATPase complexes condensin and cohesin, which are thought to form ring structures that generate chromosome super coiling or cross-linking (Haering and Nasmyth, 2003). Whereas cohesin is responsible for maintaining sister chromatid cohesion until anaphase onset, condensin I and II contribute to chromatid condensation and resolution. However, the disruption of condensin function in several different organisms did not dramatically inhibit compaction or longitudinal shortening of chromosomes, suggesting that other activities contribute to the control of mitotic chromosome length (Steffensen et al., 2001; Hagstrom et al., 2002; Hudson et al., 2003).

In addition to adopting a physical form that can be segregated effectively to generate daughter nuclei, chromosomes recruit factors that are essential for productive interactions with spindle microtubules both at their kinetochores and along their arms, such as the microtubule-based motors of the Kinesin-7 (centromere protein [CENP]-E) and Kinesin-10 (Kid chromokinesin) families, respectively (Vernos and Karsenti, 1996). Underlying structural differences between centromeric and arm chromatin are thought to help direct specific associations. For example, specialized chromatin at centromeres containing the histone H3 variant CENP-A is essential for both centromere rigidity and to recruit many downstream factors (Van Hooser et al., 2001; Black et al., 2004).

Correspondence to Rebecca Heald: heald@socrates.berkeley.edu

Abbreviations used in this paper: CAP, chromosome-associated protein; CENP, centromere protein; CSF, cytostatic factor.

The online version of this article contains supplemental material.

The Journal of Cell Biology, Vol. 169, No. 6, June 20, 2005 859–869
http://www.jcb.org/cgi/doi/10.1083/jcb.200503031

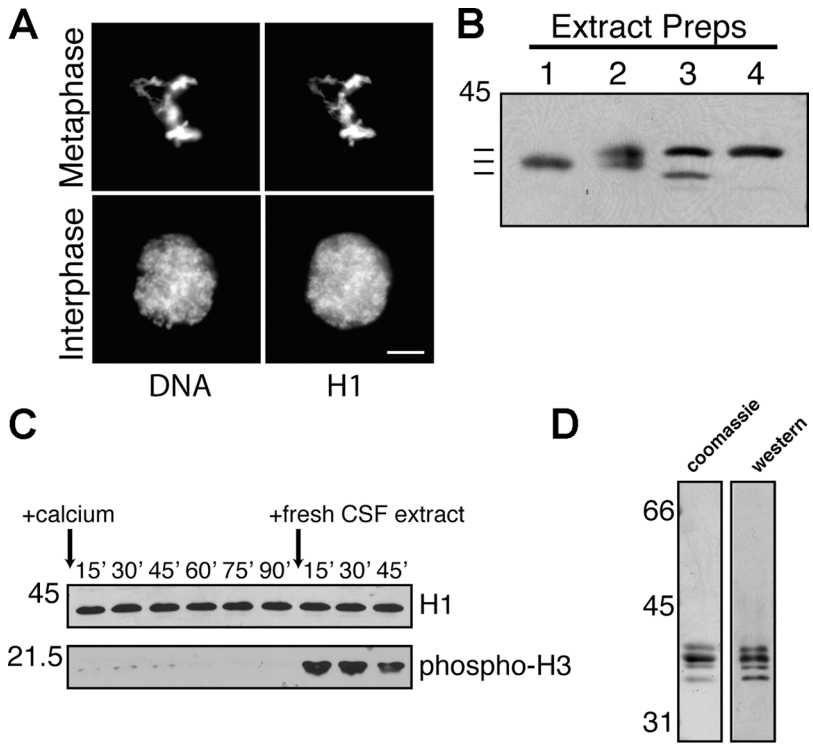

Figure 1. **Characterization of embryonic histone H1.** (A) Immunofluorescence of individual sperm nuclei in *X. laevis* egg extract reactions in metaphase and interphase, stained with affinity-purified antibodies raised to embryonic histone H1 and costained with Hoechst DNA dye to show colocalization. Bar, 10 μm. (B) Western blot of four different *X. laevis* egg extract preparations probed with H1 antibodies that show variation in molecular mass. The three lines show relative positions of three different H1 isoforms. (C) Western blot of samples collected at 15-min time intervals from a CSF egg extract induced to enter interphase by calcium addition and then back into metaphase by the addition of fresh CSF extract. H1 migration does not change during interphase and metaphase. Phospho-H3 epitopes appear only in mitotic samples. (D) Embryonic histone H1 purified from extract that was pooled from the eggs of ~20 frogs yielded at least four bands by SDS-PAGE and coomassie staining (left lane), all of which were recognized by Western blot analysis with affinity-purified H1 antibodies (right lane) and were confirmed by mass spectrometry to be embryonic H1 (not depicted). The destained gel was delivered to the Howard Hughes Medical Institute Mass Spectrometry Facility (University of California Berkeley) for protein band excision, digestion, and mass spectrometric analysis.

Linker histone H1 was once hypothesized to be an important determinant of the mitotic chromosome structure because it can stabilize the compaction of nucleosomes into a 30-nm chromatin fiber, and its hyperphosphorylation is a hallmark of mitosis in many cell types (Boggs et al., 2000; Hansen, 2002). Although classic structural studies signified an important role for H1 in overall chromatin organization (Thoma and Koller, 1977; Thoma et al., 1979), a definitive role for H1 in generating vertebrate mitotic chromosome architecture has not been established. Rather, functional studies of H1 and related proteins in multiple systems to date have indicated a role for linker histones in regulatory processes, including gene expression, chromatin accessibility, homologous recombination, and apoptosis (for review see Harvey and Downs, 2004). Mice lacking multiple H1 subtypes die by midgestation, but the cause is unknown (Fan et al., 2003). Although linker histone knockouts disrupted chromosome compaction in *Tetrahymena thermophila* (Shen et al., 1995), the dispensability of H1 for establishing chromosome structure in vertebrates was suggested by experiments in *Xenopus laevis*, as cytostatic factor (CSF)–arrested metaphase egg extracts that had been depleted of embryonic linker histone H1 supported the normal morphological condensation of unreplicated sperm chromatids (Ohsumi et al., 1993). However, the assay conditions that were applied, although frequently used to study mitotic chromosome condensation, failed to support essential features of normal genome propagation, including spindle assembly, chromosome replication, and kinetochore assembly.

Using *X. laevis* egg extracts that reconstitute the entire process of chromosome replication and segregation in vitro, we set out to investigate the contribution of linker histone H1 to the organization and activity of functional chromosomes. We show that histone H1 is enriched on duplicated chromosomes relative to CSF chromatids, and its depletion causes a dramatic lengthening of chromosomes that prevents their proper alignment and segregation. Despite arm defects, kinetochores appear to form and function properly, which is consistent with the observation that histone H1 levels appear reduced at centromeric chromatin, where CENP-A is enriched. Our results indicate that H1 is a crucial determinant of mitotic chromosome structure.

Results

Characterization of embryonic linker histone H1 in *X. laevis* egg extracts

X. laevis eggs are stockpiled with a maternal histone H1 variant known as B4 that functions as the linker histone in early embryonic cell divisions until the midblastula transition (Dworkin-Rastl et al., 1994). We generated a polyclonal antibody against recombinant B4 (hereafter referred to as H1) that specifically decorated interphase and metaphase chromatin by immunofluorescence (Fig. 1 A). A variable number of distinct H1 bands (1–4) ranging in molecular mass from 35 to 40 kD were detected by SDS-PAGE and Western blots of different extract preparations (Fig. 1 B). Heterogeneity did not result from cell cycle–dependent phosphorylation, as no differences in H1 migration were detected between interphase and mitosis (Fig. 1 C), and alkaline phosphatase treatment did not alter the migration of H1 bands (not depicted). Purification of H1 from egg extract pooled from ~20 different frogs yielded four bands that were confirmed by Western blot analysis and mass spectrometry to be embryonic H1 (Fig. 1 D). Thus, our data are consistent with previous studies indicating that multiple embryonic H1 variants exist in *X. laevis* (Dimitrov et al., 1994; Dworkin-Rastl et al., 1994).

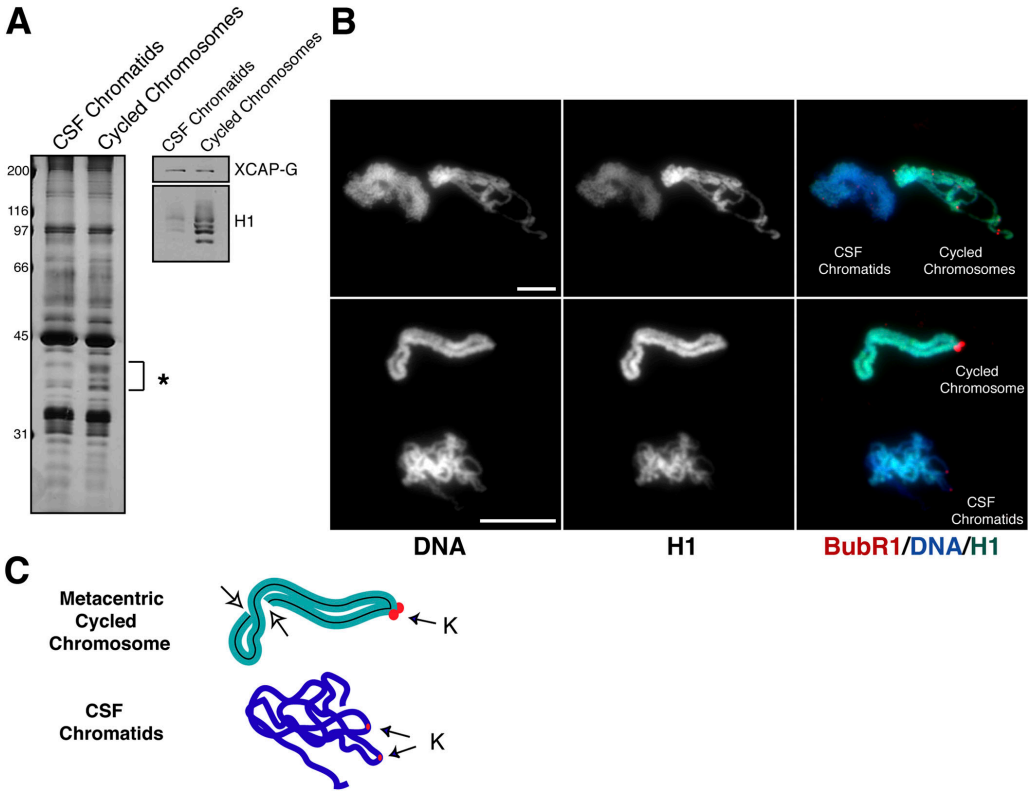

Figure 2. **CSF chromatids recruit reduced levels of histone H1.** (A) Comparison of chromatin proteins that are associated with unreplicated chromatids formed in a CSF extract with cycled mitotic chromosomes that have undergone duplication. Silver-stained gel reveals a similar protein pattern, except in the region marked by an asterisk at ~40 kD. By using Western blot analysis, we find that the proteins enriched in this region on duplicated chromosomes correspond to histone H1 bands, whereas XCAP-G levels appear similar. (B) Fluorescence images showing H1 and kinetochore marker BubR1 staining on CSF chromatids and duplicated mitotic chromosomes. Assembly reactions were fixed separately and were then pooled before isolating structures onto a coverslip and processing for immunofluorescence staining. Cycled chromosomes were discernible from CSF chromatids based on DNA morphology, BubR1staining intensity, and the presence of paired sister chromatids and kinetochores. The top panels are from one field of view containing the two types of assembled chromatin structures: CSF chromatids and cycled chromosomes, as indicated in the merged image. Each cluster contains approximately six to eight chromatids or cycled chromosomes. The bottom panels are enlarged images of another field of view showing one individual cycled chromosome next to two CSF chromatids, as indicated in the merged image. Enrichment of histone H1 on duplicated chromosomes is most clearly evident in the merged images. Bars, 10 μm. (C) Schematic diagram of the structures shown in the bottom panels of B. The top structure is a metacentric chromosome consisting of two sister chromatids, delineated by the black line and partially folded back on itself. The open arrows point to the two ends of the cycled chromosome. Based on BubR1 staining, the bottom structure likely consists of two tangled CSF chromatids. Closed arrows point to the kinetochores (K).

H1 is enriched on chromosomes that have undergone replication

Previous experiments have indicated that histone H1 is dispensable for the formation and resolution of unreplicated chromatids in CSF-arrested metaphase extracts (Ohsumi et al., 1993). To evaluate these chromatids with respect to more physiological mitotic chromosomes, we compared the protein profile and morphology of demembranated sperm nuclei that were incubated directly in CSF extracts (CSF chromatids) with those that had undergone DNA replication in interphase before cycling into metaphase (cycled chromosomes). By isolating chromatids and chromosomes from the extract, followed by analyzing their associated proteins by SDS-PAGE and silver staining, we observed that most chromatin-associated proteins (CAPs) that were detected were present at comparable levels in the two preparations, with the exception of several bands between 35 and 40 kD that were enriched on cycled chromosomes (Fig. 2 A). By using Western blot analysis, the enriched bands were revealed to be histone H1 (Fig. 2 A). Whereas H1 was recruited to CSF chromatids, increased H1 levels (4–10-fold in three independent experiments) were consistently observed on cycled chromosomes (unpublished data). In agreement with this observation, H1 was also found more highly concentrated on cycled chromosomes compared with CSF chromatids by using immunofluorescence analysis (Fig. 2 B). Although cycled chromosomes consisted of condensed and paired sister chromatids with duplicated kinetochore foci, unreplicated chromatids appeared much thinner and tangled with smaller and unpaired kinetochores (Fig. 2, B and C). Thus, cycled chromosomes accumulate histone H1 in an interphase-dependent manner and form more physiologically relevant structures than CSF chromatids.

Replicated chromosomes lacking H1 exhibit morphological defects

To investigate whether H1 contributes to the formation of normal mitotic chromosomes, a polyclonal antibody was used to immunodeplete CSF-arrested egg extracts, removing >95% of H1 as determined by Western blot analysis and indirect immunofluorescence of spindle assembly reactions (Fig. 3, A and B).

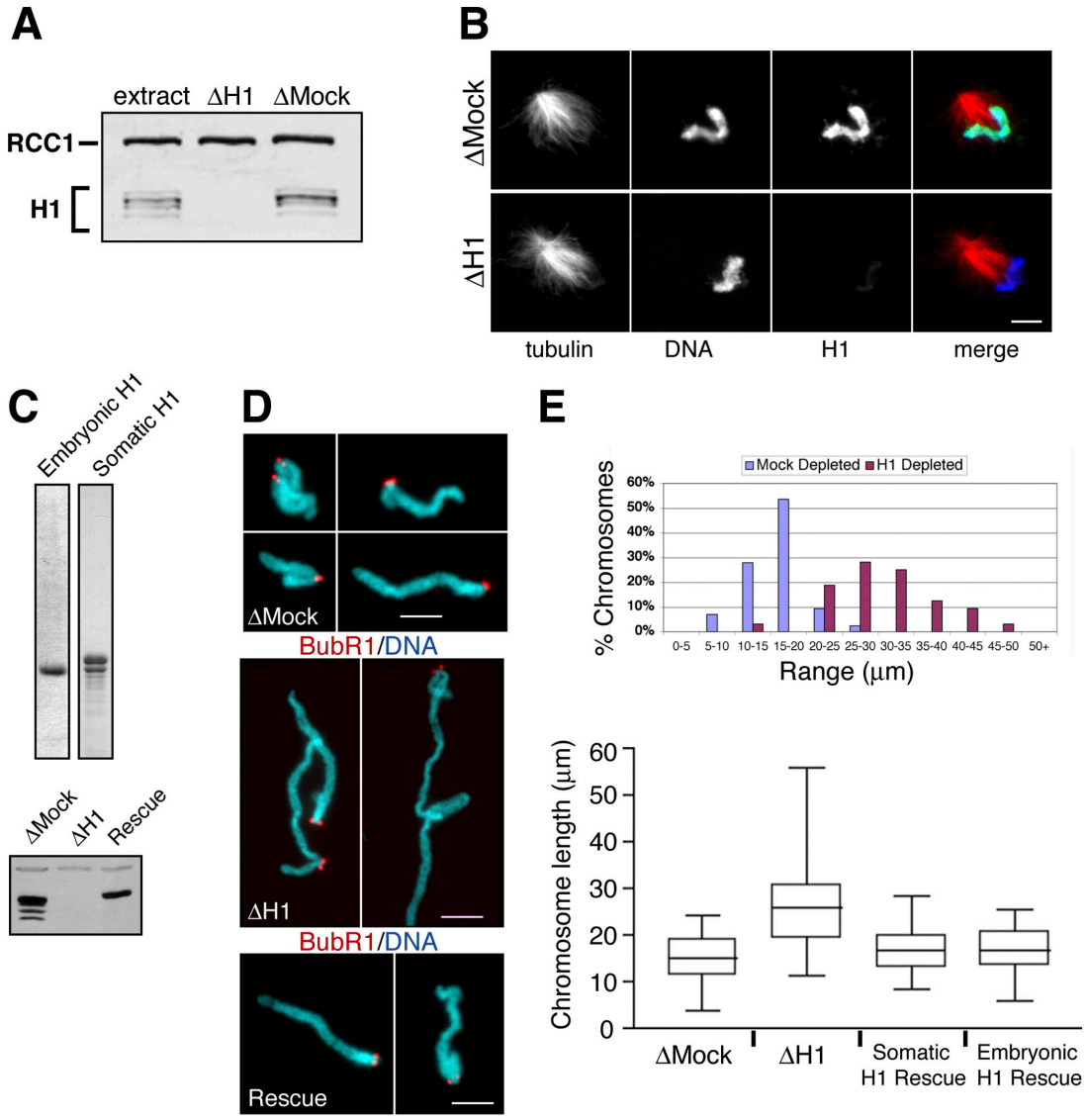

Figure 3. **Immunodepletion of H1 causes an elongated chromosome morphology.** (A) Western blot of total, H1-depleted, and mock-depleted extract probed with H1 and RCC1 antibodies to show that >95% of H1 was removed, whereas chromatin protein RCC1 was unaffected by the procedure. (B) Fluorescence images of half spindles assembled around sperm nuclei incubated in CSF extracts. Structures contain a polarized array of microtubules oriented toward the DNA, from which H1 can be efficiently depleted. In merged images, microtubules are red, DNA is blue, and H1 is green. (C) Coomassie-stained gels showing recombinant H1 purified from insect cells and somatic H1 purified from calf thymus that were used in add-back experiments. (bottom) Western blot of mock-depleted, H1-depleted, and rescue conditions with 1.5 μM of embryonic H1 added to the depleted extract. (D) Immunofluorescence of individual replicated chromosomes from mock-depleted, H1-depleted extracts, and rescued reactions in which H1-depleted extracts were supplemented with endogenous levels (1.5 μM) of purified histone H1. The same results were obtained for embryonic H1 rescues. Chromosomes were costained with Hoechst DNA dye (blue) and BubR1 antibodies (red) to label kinetochores. (E) Quantification of chromosome lengths. (top) Distribution of chromosome lengths in mock-depleted and H1-depleted extracts (mock depleted, $n = 43$; H1 depleted, $n = 35$). (bottom) Box and whiskers plot from a representative rescue experiment ($n = 62$ for each condition). The middle line of each box is the median. Top and bottom lines are the third and first quartiles, and the whiskers indicate the maximum and minimum chromosome length measurements. The elongated conformation of H1-depleted chromosomes was largely rescued by the addition of either somatic or embryonic histone H1 to H1-depleted extracts. Bars, 10 μm.

In agreement with previous results, sperm nuclei that were incubated directly in either mock- or H1-depleted CSF extracts resolved into thin, individual unreplicated chromatids that appeared morphologically similar when viewed by fluorescence microscopy (Ohsumi et al., 1993; unpublished data). In contrast, when extracts were cycled through interphase, H1-depleted chromosomes exhibited significant morphological defects that were characterized by elongated chromosome arms that often appeared kinked, buckled, and twisted (Fig. 3 D).

To further characterize and quantify the observed morphological defects caused by H1 depletion, we measured the lengths of control and H1-depleted chromosomes. Each *X. laevis* sperm nucleus contains 18 chromatids (Tymowska, 1977; Edwards and Murray, 2005), with mitotic lengths ranging from ~5 to 25 μm (Fig. 3 E). On average, H1-depleted replicated chromosomes were 50% longer than mock-depleted controls, with a broader distribution of lengths up to 50 μm (Fig. 3 E). The morphological and length defects that were observed for H1-

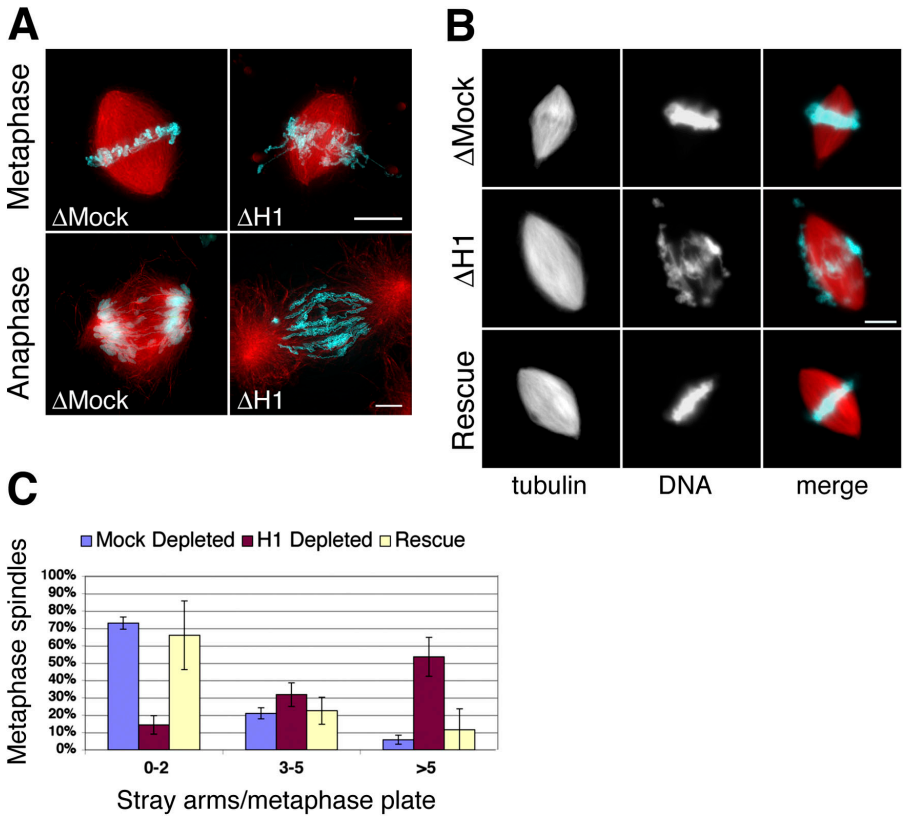

Figure 4. **H1 depletion prevents proper chromosome alignment and segregation by the mitotic spindle.** (A) Mock- and H1-depleted spindle assembly reactions containing rhodamine-labeled tubulin and stained with Hoechst DNA dye reveal that chromosomes cannot align properly in metaphase in the absence of H1 and are not effectively segregated during anaphase. (B) Fluorescence images of metaphase spindles showing that chromosome alignment defects caused by H1 depletion can be rescued by the readdition of somatic H1 to 1.5 μM. In merged images, microtubules are red and DNA is blue. (C) Quantification of chromosome alignment defects. The number of arms that had strayed from the metaphase plate were counted in mock- and H1-depleted spindles and in H1-depleted spindle reactions supplemented with purified H1 (mock depleted, $n = 459$; H1 depleted, $n = 448$; rescue, $n = 165$). The percentages of metaphase spindles with 0–2, 3–5, and >5 misaligned arms are shown. Error bars represent SD. Bars, 10 μm.

depleted chromosomes could be largely rescued by the addition of either purified embryonic or somatic H1 to depleted extracts at endogenous levels (~1.5 μM), indicating that H1 was the only relevant activity depleted by the antibody (Fig. 3, C–E). Thus, histone H1 is required for replicated interphase chromatin to fully compact into normal metaphase chromosomes.

H1-depleted chromosomes cannot be properly aligned or segregated

Considering that a significant percentage of H1-depleted chromosomes were actually longer than a typical metaphase spindle assembled in egg extracts (~30 μm), we investigated the behavior of histone H1-depleted chromosomes in the context of the spindle apparatus. Extracts that were supplemented with rhodamine-labeled tubulin were monitored by fluorescence microscopy as they progressed through the cell cycle. As observed previously, the absence of H1 did not appear to interfere with nuclear assembly or with DNA replication during interphase (Dasso et al., 1994; unpublished data). Spindles formed normally in both control and H1-depleted reactions upon entry into metaphase. However, "stringy" and elongated H1-depleted chromosomes failed to align properly at the metaphase plate and were often observed dangling outside of the spindle (Fig. 4 A). Furthermore, H1-depleted reactions displayed dramatic defects during anaphase, as chromosomes failed to clear the middle of elongating anaphase spindles (Fig. 4 A).

To quantify the chromosome misalignment defects, we counted the number of chromosome arms that failed to align onto the metaphase plate in each bipolar spindle. In five separate experiments, a mean of 54% of H1-depleted metaphase spindles possessed greater than five misaligned chromosome arms, compared with only 6% in mock-depleted controls (Fig. 4 C). Effects of H1 depletion were largely rescued by adding back purified H1, yielding 12% of spindles with greater than five misaligned arms (Fig. 4, B and C). In control and rescue reactions, 73 and 66% of structures, respectively, exhibited tight metaphase alignment (zero to two arms misaligned) compared with only 14% of structures in H1-depleted reactions (Fig. 4 C). The rescue of both chromosome length and metaphase alignment in add-back experiments indicates that the role of H1 in determining chromosome length is an essential function for proper alignment and anaphase segregation.

The localization of other chromosomal proteins is not dramatically altered on H1-depleted chromosomes

The morphological and functional defects observed when histone H1 was depleted from chromosomes could reflect a direct role for H1 in normal chromatin fiber compaction. Alternatively, defects could result from secondary effects caused by the mislocalization of other chromosomal regulators in the absence of H1. To investigate these possibilities, control and H1-depleted chromosomes were purified by centrifugation through a sucrose cushion, and their CAP profiles were analyzed by SDS-PAGE and silver staining. Other than the absence of histone H1, there were no dramatic differences in the profile and relative abundance of detectable CAPs, including core histones, that were associated with mock and H1-depleted chro-

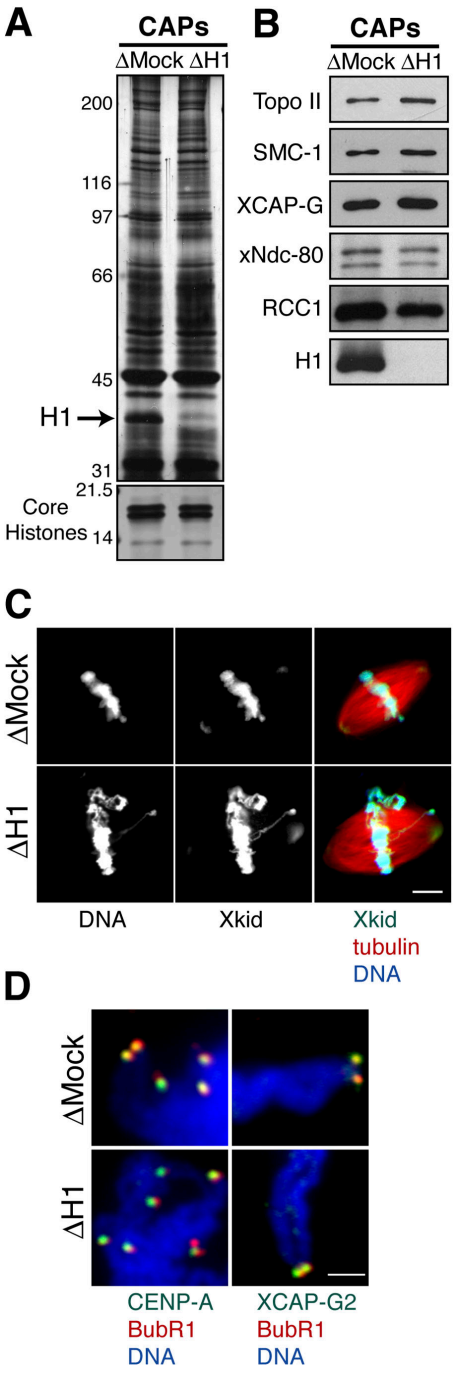

Figure 5. **Other chromosomal proteins bind at similar levels in the absence of histone H1.** (A) Chromosome-associated protein (CAP) profiles of cycled chromosomes isolated from mock- and H1-depleted extracts and analyzed by SDS-PAGE and silver staining. (bottom) Core histones of the same sample run on a higher percentage gel. Note that the only apparent difference between the two samples is a band at the molecular mass of H1. (B) Western blot analysis of mock- and H1-depleted CAPs. Blots were probed with antibodies to topoismerase II, cohesin subunit SMC-1, condensin subunit XCAP-G, kinetochore component Ndc80, RanGEF RCC1, and histone H1. H1 is the only CAP observed to be absent after H1 depletion. (C) Immunofluorescence analysis of Kinesin-10 (Xkid) in mock- and H1-depleted spindles. In the merged image, microtubules are red, DNA is blue, and Xkid is green. Although H1 depletion impairs chromosome alignment, Xkid localization is not affected. Bar, 10 μm. (D) Immunofluorescence analysis showing similar localization of kinetochore proteins on mock- and H1-depleted chromosomes. Left panels show histone H3 variant CENP-A (green) and BubR1 (red), and right panels show condensin II subunit XCAP-G2 (green) and BubR1 (red). DNA is blue. Bar, 2.5 μm.

mosomes (Fig. 5 A). By using Western blot analysis, a number of well-characterized CAPs were found at comparable levels in both control and H1-depleted chromosome fractions, including topoisomerase II-α, XCAP-G (condensin I component), SMC-1 (cohesin component), RCC1 (Ran GEF), Kinesin-6 (XKLP1), and the kinetochore component xNdc80 (Fig. 5 B and not depicted). We also examined the localization of a number of CAPs by analyzing immunofluorescence of cycled chromosomes. Of particular interest were the chromokinesins XKLP1 and Xkid, whose mislocalization could lead to chromosome alignment defects. Both were found to localize similarly on H1- and control-depleted metaphase chromosomes by immunofluorescence (Fig. 5 C and not depicted). Kinetochore proteins also appeared morphologically normal in the absence of H1. BubR1 and CENP-A colocalized at discrete sites corresponding to kinetochores on both mock- and H1-depleted chromosomes (Fig. 5 D). Furthermore, the condensin II–specific component XCAP-G2 also appeared strongly enriched at kinetochores under both conditions, largely colocalizing with BubR1 (Fig. 5 D). These data indicate that the morphological and functional chromosome defects seen upon H1 depletion are a direct result of the loss of H1 function, rather than a secondary defect caused by a dramatic mislocalization of other CAPs such as cohesins, condensins, chromokinesins, or kinetochore components. However, we cannot rule out that subtle changes in chromatin protein levels or alterations of their activities caused by H1 depletion may contribute to the observed defects.

Functional kinetochores form in the absence of H1

Although kinetochores appeared to form normally in the absence of histone H1, the loss of kinetochore function could also contribute to the observed chromosome alignment and segregation defects. However, several lines of evidence suggested that kinetochores were functional in the absence of H1. In metaphase, we observed that the kinetochores, which were marked by CENP-A staining, often clustered at the metaphase plate despite failures in chromosome arm congression (Fig. 6 A). Furthermore, although chromosome arms failed to segregate effectively during anaphase in the absence of H1, discrete points on each chromosome were still drawn toward spindle poles, indicative of functional microtubule attachments at kinetochores (Fig. 4 A). Therefore, we hypothesized that functional kinetochores were assembled in the absence of H1.

Hallmarks of kinetochore functionality are microtubule attachment and directed chromosome movement. To better visualize and compare these functions in the presence and absence of H1, we added the spindle Kinesin-5 (Eg5) inhibitor monastrol, which causes metaphase spindles to form rosette structures that are characterized by collapsed poles surrounded by a ring of chromosomes (Mayer et al., 1999; Kapoor et al., 2000). Functional kinetochores attach to microtubules and orient toward the center of these monoasters (Ono et al., 2004). Kinetochores labeled with CENP-A antibodies successfully attached and oriented toward the center of monastrol rosettes in both control and H1-depleted chromosomes, indicating that loss of H1 did not impair kinetochore-mediated microtubule attachment and

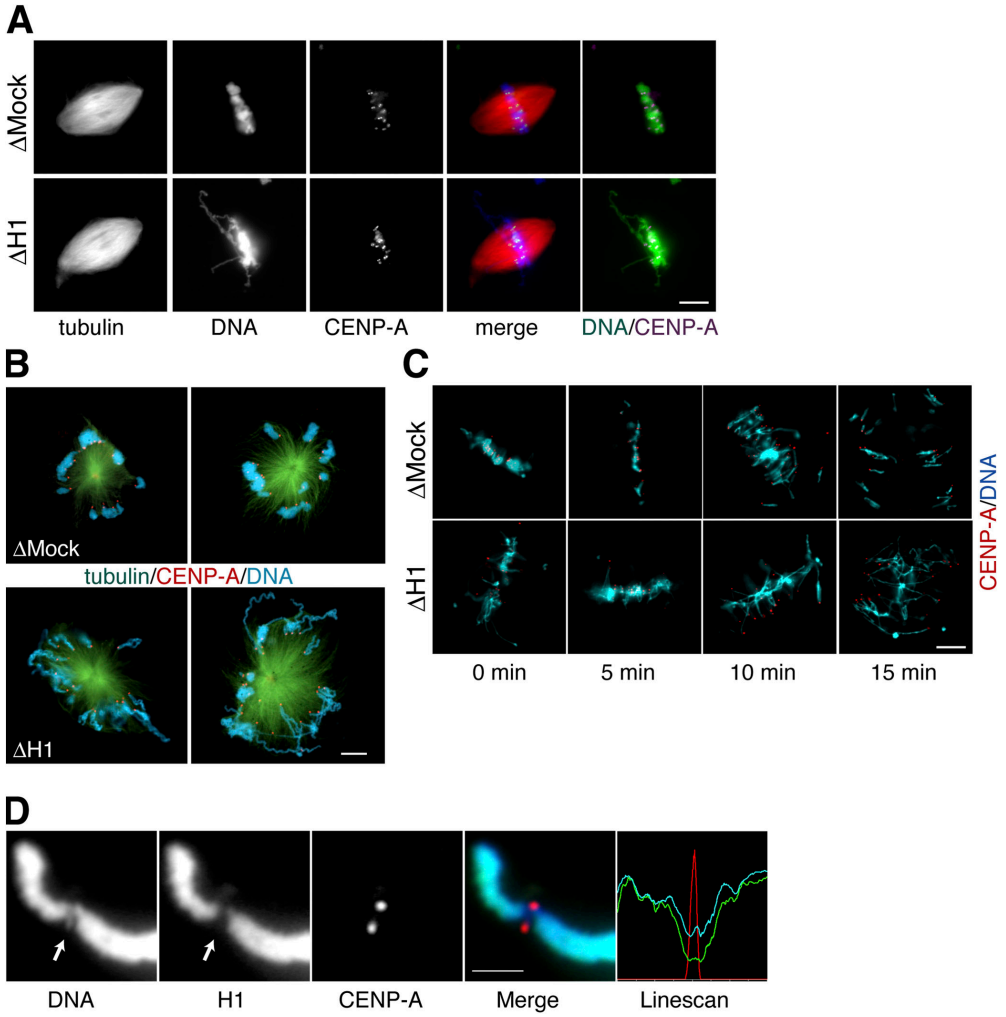

Figure 6. **Kinetochores appear to function normally in the absence of histone H1.** (A) Kinetochores visualized by CENP-A immunofluorescence localize to the metaphase plate despite misalignment of chromosome arms in the absence of H1. In the merged image, microtubules are red, DNA is blue, and CENP-A is green. The DNA/CENP-A merged image is meant to further highlight the observed metaphase clustering of CENP-A despite arm misalignment. DNA is green and CENP-A is purple. Bar, 10 μm. (B) Kinetochores attach and orient similarly in mock- and H1-depleted spindles treated with Eg5 inhibitor monastrol. Note CENP-A staining (red) on discrete kinetochores that were attached to microtubules and were oriented toward the center of monoaster structures. Microtubules are green and DNA is blue. Bar, 10 μm. (C) Kinetochores segregate during anaphase in the absence of H1. Samples from mock- and H1-depleted spindle reactions induced to enter anaphase were fixed at 5-min intervals. Kinetochores visualized by the addition of directly labeled CENP-A antibodies segregate similarly in both reactions, whereas chromosome arms (blue) are elongated and tangled in the absence of H1. Bar, 10 μm. For time-lapse videos of kinetochore segregation in the presence and absence of H1, see Videos S1 and S2 (available at http://www.jcb.org/cgi/content/full/jcb.200503031/DC1). (D) Duplicated *X. laevis* sperm chromosomes stained with antibodies to histone H1 (green), CENP-A (red), and Hoechst DNA dye (blue). Linescan shows relative intensity of staining along the length of the chromosome. Note the lack of H1 signal on centromeric DNA nubbin (arrows). Bar, 2.5 μm.

movement (Fig. 6 B). To confirm that chromosome segregation could occur despite the arm defects of H1-depleted chromosomes, we visualized kinetochores shortly after anaphase induction by both fixation and time-lapse microscopy of spindles in the presence of fluorescently labeled CENP-A antibody (Fig. 6 C; see Videos S1 and S2, available at http://www.jcb.org/cgi/content/full/jcb.200503031.DC1; Maddox et al., 2003). There was no obvious difference in the movement of kinetochores in control and H1-depleted anaphase reactions. Therefore, defects in the alignment and segregation of H1-depleted chromosomes are not caused by a lack of functional kinetochores, but likely result from the physical and structural abnormalities of chromosome arms assembled in the absence of H1.

Our results indicate a critical role for H1 in defining chromosome arm architecture but indicate dispensability for kinetochore function. Interestingly, sequence analysis of centromeric histone H3 variant CENP-A has revealed the presence of short, conserved basic motifs that are often found on linker histone tails, suggesting that CENP-A could associate with linker DNA at the centromere in place of H1 (Malik et al., 2002). Consistent with this hypothesis, we consistently observed reduced levels of linker histone H1 at CENP-A–staining centromeric regions and at the inner centromeres of metaphase chromosomes (Fig. 6 D). These observations raise the possibility that H1 and CENP-A localizations are mutually exclusive and may help define distinct mitotic chromosomal domains.

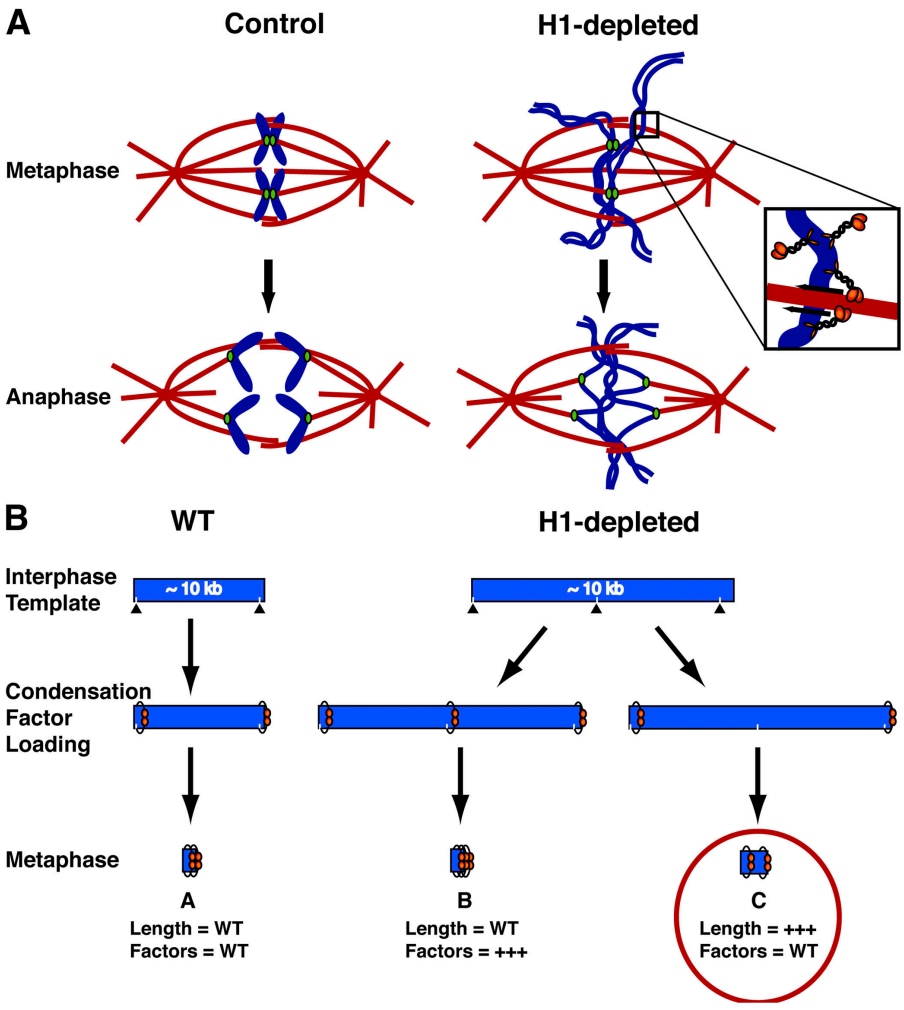

Figure 7. **Schematics illustrating the potential role of histone H1 in chromosome condensation, alignment, and segregation.** (A) Illustration comparing *X. laevis* spindles and chromosomes in metaphase and anaphase in the presence or absence of H1. Note that the kinetochores align and segregate normally in both mock- and H1-depleted conditions. H1-depleted chromosome arms do not align properly as a result of their elongated conformation. Inset highlights how elongated chromosomes would have productive microtubule–chromokinesin interactions within the confines of the spindle but not when dangling outside. H1-depleted chromosomes do not segregate properly as a result of their extended length and the presence of twisted and tangled chromatids that remain in the center of the spindle. (B) A closer analysis of H1-depleted interphase chromatin length and condensation factor levels could differentiate between two potential mechanisms of condensation factor deposition onto the chromatin template. Scenario A represents the compaction of a wild-type interphase fiber by condensation factors. Scenarios B and C assume the H1-depleted interphase chromatin template is physically longer than the wild-type template. If condensation factors are deposited at specific physical distances along the chromatin template (schematically represented by triangles and hatchmarks), then mitotic chromosome length might be normal (scenario B) in H1-depleted chromosomes. Regardless of the effect on metaphase length, scenario B would lead to increased levels of condensation factors on H1-depleted chromosomes. However, if the distribution of condensation machinery is defined at the level of the DNA template (~10 kb), then compaction of H1-depleted interphase chromatin would generate longer metaphase chromosomes with the same level of condensation factors as wild-type chromosomes (scenario C). Our data support scenario C.

Discussion

Histone H1 is required for mitotic chromosome compaction, alignment, and segregation

Our data provide the first direct demonstration of a role for histone H1 in vertebrate mitotic chromosome structure. Although evidence exists supporting a role for linker histone in ciliate chromosome compaction (Shen et al., 1995), the prevailing view has been that H1 variants in vertebrates fulfill other roles in modulating chromatin accessibility, gene expression, and other processes (Harvey and Downs, 2004). Given its fundamental role in defining lower order chromatin organization, it seemed likely that H1 would also contribute to mitotic chromosome architecture. However, elucidating a structural role for H1 in chromosome assembly in mammalian systems is complicated by the presence of multiple H1 isoforms. The knockout of multiple H1s in mice caused embryonic lethality (Fan et al., 2003), and it will be interesting to ascertain whether chromosome segregation defects contributed to this phenotype. Simultaneous RNA interference depletion of multiple isoforms may also reveal whether H1 functions in chromosome architecture in other systems and cell types.

In the absence of H1 in *X. laevis* egg extracts, mitotic chromosomes assume an elongated confirmation and fail to align during metaphase or segregate properly during anaphase (Fig. 7 A). We believe that the elongated nature of H1-depleted chromosome arms is the direct cause of the observed defects for two major reasons: (1) rescue conditions that restore chromosome length also restore metaphase alignment; and (2) chromosomal components, including kinetochores and chromokinesins, appear to localize and function normally on H1-depleted chromosomes.

How and why does chromosome length affect chromosome alignment and segregation? H1-depleted chromosome arms were often observed well outside the spindle. Perhaps they could not be aligned despite normal chromokinesin localization simply because the interaction between chromosomes and microtubules did not occur (Fig. 7 A, inset). Thus, one primary function of chromosome compaction may be to facilitate productive chromokinesin activity by increasing chromatin–microtubule contacts. During anaphase, chromosomes that were longer than the spindle itself could not be effectively segregated. Furthermore, we also observed H1-depleted chromatids twisting around one another, which would make them difficult to resolve. In addition to chromosome length, it is

possible that other physical traits of chromosomes are altered in the absence of H1, such as rigidity or elasticity. In the future, biophysical studies of individual chromatin molecules and chromosomes will be essential to better understand the interplay between the structure and physical properties of chromosomes and their behavior within the mitotic apparatus.

CSF chromatids versus cycled chromosomes

A role for histone H1 in mitotic chromosome architecture was previously discounted when it was demonstrated that H1 was dispensable for the normal condensation of unreplicated chromatids in clarified CSF *X. laevis* egg extracts (Ohsumi et al., 1993). In contrast, we have found that histone H1 is essential for the proper compaction of duplicated interphase chromosomes into their metaphase configuration in crude cycled extracts. These observations are not necessarily contradictory, as we observed that H1 is significantly enriched on cycled chromosomes relative to CSF chromatids. Although our reactions in crude CSF extract do not precisely reproduce the experimental conditions of Ohsumi et al. (1993), we propose that CSF chromatids assembled in either crude or clarified extract are less sensitive to H1 depletion because they are partially depleted of H1 relative to the more physiologically relevant cycled chromosomes. In fact, CSF chromatids often resemble H1-depleted chromosomes in their extended length and thin, tangled morphology. Thus, our data indicate that entry into an interphase state facilitates the full enrichment of H1 onto chromatin. H1 loading could be promoted in several ways: (1) nuclear assembly and import could allow for local enrichment of H1 in the vicinity of chromatin; (2) the decondensed interphase template could be more accessible to H1; and (3) H1 may be loaded in a replication-dependent/assisted fashion. It will be interesting to further investigate the dynamics and regulation of H1–chromatin association during the cell cycle by using the egg extract system.

Elongated chromosomes and the mitotic compaction machinery

Why are H1-depleted chromosomes ~50% longer than normal metaphase chromosomes? Based on previous studies of the role of H1 in interphase chromatin (Thoma et al., 1979; Boggs et al., 2000; Woodcock and Dimitrov, 2001; Hansen, 2002), we hypothesize that depleting H1 from extracts destabilizes the 30-nm fiber, generating an elongated interphase chromatin template that, upon compaction in mitosis, leads to longer chromosomes. We envisage two major pathways by which the condensation machinery could be loaded onto interphase chromatin, resulting in differences in mitotic chromosome compaction (Fig. 7 B). Factors such as condensin could be loaded either at intervals defined by the physical length of the interphase template (e.g., at 10-nm periodicity along chromatin) or at specific DNA-defined intervals (e.g., every 10 kb). If condensation factors were deposited at specific physical distances along the interphase template, then more condensation machinery would be loaded onto the longer H1-depleted template. In contrast, if deposited at DNA-defined intervals, condensation factors would be spaced farther apart on the H1-depleted template and could lead to increased chromosome length in metaphase despite the presence of normal levels of condensation machinery. The fact that we observe comparable levels of known condensation factors such as condensin I and topoisomerase II on both mock- and elongated H1-depleted chromosomes favors the idea that the deposition of these factors is defined at the level of DNA kilobases rather than by the physical length of the template. Deposition of chromatin condensation and cohesion factors at defined DNA intervals is supported by biophysical studies and chromosome immunoprecipitation experiments (Earnshaw et al., 1985; Kimura and Hirano, 1997; Laloraya et al., 2000; Poirier and Marko, 2002; Hudson et al., 2003; Glynn et al., 2004). Undertaking a thorough quantitative comparison of interphase chromatin lengths and condensation factor levels in control and H1-depleted chromosomes will help to distinguish between these models of chromosome condensation. Furthermore, the addition of purified H1 to depleted extracts at various time points in the chromosome cycle may more directly address when and how H1 contributes to chromosome compaction.

H1 and CENP-A may define local structural environments along the chromosome

Our data show that kinetochores can assemble and function despite the structural defects induced by H1 depletion, suggesting that linker histone H1 is not a crucial determinant of centromere function. Preliminary experiments suggest that H1 is largely excluded from centromeres, where the histone H3 variant CENP-A is enriched (Fig. 6 D and not depicted). Interestingly, recent findings suggest that CENP-A–containing nucleosomes could confer a structural rigidity to centromeric chromatin that spatially defines and maintains functional centromeres (Black et al., 2004). Thus, the structurally and functionally distinct domains of arm and centromeric chromatin are likely defined by the local deposition of core components like H1 and CENP-A. Differences between these two domains are highlighted by the dissimilar localization of other factors along vertebrate chromosomes such as condensin I and II (Ono et al., 2003, 2004), as well as the distinct physical and functional characteristics of centromeres and flanking heterochromatin observed in many systems, such as *Drosophila melanogaster* (Blower and Karpen, 2001). Defining the structural environments of chromosome arms and centromeres and the interplay among their resident factors is of significant interest.

Ultimately, the purpose of mitotic chromosome condensation and organization is to ensure that segregation of the genome occurs with high fidelity during cell division. Linker histones were thought to be nonessential for these critical processes. On the contrary, our data indicate that linker histones are required for proper mitotic chromosome condensation by contributing to arm architecture. We hypothesize that the loss of H1 function in vivo may potentiate aneuploidy as a result of defects in chromosome condensation and an increased likelihood of chromosome missegregation events in mitosis.

Materials and methods

X. laevis egg extracts, in vitro spindle, and chromosome assembly

Crude CSF extracts were prepared from *X. laevis* eggs as described previously (Murray, 1991; Wignall et al., 2003). To assemble metaphase spindles and replicated chromosomes, CSF extracts were supplemented with demembranated sperm nuclei (500 nuclei/μl) and transferred to a 20°C water bath. After a 15-min incubation, 0.1 vol $CaCl_2$ solution (4 mM $CaCl_2$, 10 mM Hepes, pH 7.7, 150 mM sucrose, 100 mM KCl, and 1 mM $MgCl_2$) was added to reactions to release the extract into interphase, allowing nuclear formation and DNA replication. After 90 min, an equal volume of CSF-arrested extract (without sperm) was added to reactions to drive the extract into metaphase. Metaphase spindles with aligned replicated chromosomes generally formed after 45–60 min. To induce anaphase, an additional 0.1 vol $CaCl_2$ solution was added to cycled reactions containing metaphase spindles. Spindles were visualized by supplementing the extract with X-rhodamine–labeled tubulin (50 μg/ml).

Histone H1 purifications from insect cells and _X. laevis_ egg extract

To generate recombinant H1 for add-back experiments, the coding sequence of the B4 (*X. laevis* embryonic H1) gene was transferred from a pGEX.KG construct (gift of M. Dasso, National Institutes of Health, Bethesda, MD) into FastBac HT-A vector (Invitrogen) by using XhoI and NcoI restriction sites to create the construct BF-02, and it was confirmed by sequencing to encode H1 with an NH_2-terminal 6XHis-tag. The construct was used with the Bac-to-bac expression kit to create baculovirus BF-01. Sf9 cells infected with this baculovirus produced the 35-kD His-H1 protein product, which was confirmed by anti-H1 Western blot analysis. To purify recombinant H1, infected Sf9 cells were pelleted, subjected to a freeze/thaw cycle, and resuspended in 5 ml PBS/500 mM NaCl with protease inhibitors. The cells were further lysed by dounce homogenization and were centrifuged at 14,000 rpm for 30 min. The His-H1 protein was purified from the clear supernatant by using a nickel–nitrilotriacetic acid agarose matrix according to the manufacturer's instructions (QIAGEN). 500 mM NaCl was present in all buffers, and the eluted protein was dialyzed into PBS/500 mM NaCl and flash frozen at a high concentration (300 μM of protein).

Endogenous embryonic H1 was purified from *X. laevis* extract based on a previously described protocol for isolating H1 from *D. melanogaster* embryonic extracts (Croston et al., 1991), with the following modifications. Crude extracts were partially clarified by ultracentrifugation in a rotor (model TLS-55; Beckman Coulter) for 45 min at 4°C, followed by the removal of the cytoplasmic layer with an 18-gauge needle and 1-ml syringe. 15 ml of clarified extract was pooled before bringing the volume up to 50 ml with buffer AB. The supernatant from a 0.36-M ammonium sulfate precipitation was then syringe filtered and loaded onto a preequilibrated HiTrap Phenyl FF (high substituted) 5-ml column (Amersham Biosciences) with a peristaltic pump and was washed with 10-column volumes of HEMG-A. Once loaded and washed, the HiTrap column was transferred to an ÄKTA purifier system (model FPLC; Amersham Biosciences), and bound proteins were eluted into 1-ml fractions with a linear gradient of 2.1–0.1 M ammonium sulfate over five-column volumes. The fractions found to contain H1 by Western blot analysis (19–27) were pooled and dialyzed overnight into HEG-A buffer. The dialyzed sample was loaded onto a preequilibrated Mono S HR 5/5 column by using a super loop on the ÄKTA FPLC system, and bound proteins were eluted into 1-ml fractions with a linear gradient of 0.1–1 M KCl over 10-column volumes. H1 eluted off the Mono S HR 5/5 column at ~0.5 M KCl, as confirmed by Western blot analysis, in fractions 9 and 10. The pure fractions were pooled, concentrated, and dialyzed into PBS and 0.01% NP-40. The four bands that were present in the final fraction were each confirmed to be H1 by mass spectrometry. To avoid retention of the highly basic H1 protein on glassware, 0.01% NP-40 was included in all buffers used after the HiTrap column elution. Because *X. laevis* embryonic H1 lacks tryptophan (W) and tyrosine (Y) residues and will not absorb at UV280, a UV220 trace was also used to track the elution of H1 from the Mono S HR 5/5 column.

Antibody production

Escherichia coli BL21(DE3)pLysS cells were transformed with a pGEX-B4 plasmid (provided by M. Dasso, and referred to as H1). The GST fusion protein was purified as previously described (Dimitrov et al., 1993) from inclusion bodies, renatured, and sent to Covance Research Products, Inc. for the generation of rabbit polyclonal antibody. Antibodies were affinity purified from the serum by successive rounds of incubation, first with a GST Affi-Gel 10 (Bio-Rad Laboratories) matrix to clear all GST-specific antibodies from the serum, followed by incubation with a GST-H1 Affi-Gel 10 matrix to isolate α-H1–specific antibodies.

H1 immunodepletion, phenotype quantification, and rescues

To immunodeplete histone H1, 55 μl CSF extract was subjected to two successive 45-min incubations with 20 μg of either α-H1 (ΔH1) or control antibodies (Δmock) coupled to protein A Dynabeads (Dynal). Depletion with either random rabbit IgG or α-GST yielded identical results and are referred to throughout as Δmock. All depletions were performed on ice and before the extract was supplemented with sperm nuclei. Sperm nuclei do not contain detectable levels of linker histone H1.

To quantify the chromosome length phenotype, mock- and H1-depleted chromosomes were isolated onto coverslips before visualizing kinetochores and DNA by fluorescence staining. Individual replicated chromosomes (50–100 per condition), as determined by the presence of paired sisters and kinetochores, were then imaged at 100×, and the lengths were measured using the line and 100× calibration (previously defined with a micrometer) functions in Metamorph. The data was then transferred to Microsoft Excel and processed.

Titrations of purified embryonic H1 into depleted extract revealed that 1.5 μM gave the best phenotypic rescue and matched endogenous levels by Western blot analysis. Thus, all rescues were performed by adding back recombinant embryonic or purified somatic (Roche) H1 in PBS at a final concentration of 1.5 μM to the extract. To control for potential buffer effects, Δmock reactions in each rescue experiment were supplemented with the same volume (generally 1:30 dilution) of PBS, generating a final NaCl concentration in every reaction condition of ~5 mM.

Immunofluorescence and microscopy

To visualize metaphase/anaphase spindles, 40 vol of spindle fixative (1× BRB80, 30% glycerol, 0.1% Triton X-100, and 2.5% formaldehyde) was added to cycled reactions. After 20 min at RT, the fixation mixture was overlaid onto a 5-ml cushion (1× BRB80 and 40% glycerol) and spun onto coverslips at 6,000 rpm in a rotor (model HB-6; Sorvall) for 20 min. To better preserve chromosome structure, the same protocol as described above was used but with a different fixation solution (1× XBE2, 0.1% Triton X-100, and 2.5% formaldehyde) and cushion (1× XBE2 and 30% glycerol; Losada et al., 2000; Wignall et al., 2003). After spinning, coverslips were incubated for 5 min in −20°C methanol, washed four times with PBS and 0.1% NP-40, and blocked overnight in 3% BSA in PBS. Structures were stained with primary antibody against BubR1 (a gift of D. Cleveland, University of California, San Diego, La Jolla, CA) as previously described (Mao et al., 2003) or antibodies against histone H1 (1 μg/ml), XCAP-G2 (1 μg/ml; provided by T. Hirano, Cold Spring Harbor Laboratories, Cold Spring Harbor, NY), Xkid (1 μg/ml; gift of I. Vernos, European Molecular Biology Laboratory, Heidelberg, Germany), CENP-A (2 μg/ml; provided by A. Straight, Stanford University, Palo Alto, CA) conjugated to Alexa-594 (Molecular Probes), and H1 (1 μg/ml) conjugated to Alexa-488 (Molecular Probes). After incubating with primary antibodies, we washed coverslips four times with PBS–NP-40 and incubated them for 45 min with the appropriately labeled secondary antibodies when necessary. Coverslips were washed again, and DNA was stained with 10 μg/ml Hoechst 33258 in PBS–NP-40 for 1 min. Coverslips were mounted in Vectashield mounting media (Vector Laboratories) after a final round of washes.

Most images were acquired by using a fluorescence microscope (model E600; Nikon) equipped with a cooled CCD camera (model Orca II; Hamamatsu; at −60.0°C), shutter controller (model Lambda 10-2; Sutter Instrument Co.), and Metamorph software (Universal Imaging Corp.). Objectives were 40× dry (N.A. 0.75; Olympus), 60× oil (N.A. 1.4; Olympus), and 100× oil (N.A. 1.3; Olympus). Spindle images shown in Fig. 4 A were acquired using a deconvolution microscope (model DeltaVision Spectris DV4; Applied Precision Inc.) featuring API Softworx and SVI Huygens deconvolution software. All image files were imported into Adobe Photoshop for processing.

Chromosome isolation

50 μl Δmock or ΔH1 extract was supplemented with 5,000 sperm nuclei/μl before cycling. After assembling metaphase structures, a final volume of 100 μl of extract containing 2,500 nuclei/μl was diluted with 800 μl of chilled XBE2, leupeptin, pepstatin, chymostatin, and 0.1% Triton X-100 and was kept on ice for 15 min. The mixture was overlaid onto 2.25 ml of cushion (30% sucrose in XBE2, leupeptin, pepstatin, chymostatin, and 0.1% Triton X-100) and was spun in a HB-6 rotor at 11,000 rpm for 20 min. After removing the supernatant, the chromosomal pellet was resuspended into 40 μl of sample buffer, and 8–13 μl (~50,000–85,000 nuclei) was loaded onto an SDS-PAGE gel for Western blot analysis or silver

staining. All Western blots were probed with antibodies diluted into a 5% milk solution at final concentrations between 0.1 and 1 mg/ml. Ndc80 antibody was provided by T. Stukenberg (University of Virginia, Charlottesville, VA), Xklp1 antibody was provided by I. Vernos, and the topoisomerase II antibody was provided by T. Hirano. CSF chromatid–associated proteins were isolated as described for cycled chromosomes, but from 100 μl CSF reactions supplemented with 2,500 nuclei/μl that were incubated for 1–2.5 h. Twofold more CSF chromatid CAP samples was loaded when comparing the profile of CSF and cycled CAPs because cycled chromosomes had undergone a round of replication.

Online supplemental material

Supplemental material shows a time-lapse fluorescence video microscopy of kinetochore movements that are visualized by the addition of a directly labeled CENP-A antibody to mock-depleted (Video S1) or histone H1-depleted (Video S2) extracts containing spindles that are induced to enter anaphase. Online supplemental material is available at http://www.jcb.org/cgi/content/full/jcb.200503031/DC1.

We thank A. Fischer for her help with Sf9 insect cell culture and infection. We extend special thanks to S. Zhou for her detailed sequencing of H1 bands. We acknowledge the gift of antibodies from T. Hirano (XCAP-G2), D. Cleveland (BubR1), T. Stukenberg (Ndc80), A. Straight (CENP-A), and I. Vernos (Xkid and Xklp1). We thank M. Dasso for the GST-B4 expression vector. We also thank M. Blower, G. Karpen, and M. Eckerle for helpful centromere discussions and preliminary experiments. The authors are also extremely grateful to all members of the Heald, Weis, and Welch labs, past and present, for thoughtful discussions and support.

R. Heald is supported by the National Institutes of Health (grant GM057839).

Submitted: 7 March 2005
Accepted: 17 May 2005

References

Black, B.E., D.R. Foltz, S. Chakravarthy, K. Luger, V.L. Woods Jr., and D.W. Cleveland. 2004. Structural determinants for generating centromeric chromatin. *Nature.* 430:578–582.

Blower, M.D., and G.H. Karpen. 2001. The role of *Drosophila* CID in kinetochore formation, cell-cycle progression and heterochromatin interactions. *Nat. Cell Biol.* 3:730–739.

Boggs, B.A., C.D. Allis, and A.C. Chinault. 2000. Immunofluorescent studies of human chromosomes with antibodies against phosphorylated H1 histone. *Chromosoma.* 108:485–490.

Cleveland, D.W., Y. Mao, and K.F. Sullivan. 2003. Centromeres and kinetochores: from epigenetics to mitotic checkpoint signaling. *Cell.* 112:407–421.

Croston, G.E., L.M. Lira, and J.T. Kadonaga. 1991. A general method for purification of H1 histones that are active for repression of basal RNA polymerase II transcription. *Protein Expr. Purif.* 2:162–169.

Dasso, M., S. Dimitrov, and A.P. Wolffe. 1994. Nuclear assembly is independent of linker histones. *Proc. Natl. Acad. Sci. USA.* 91:12477–12481.

Dimitrov, S., G. Almouzni, M. Dasso, and A.P. Wolffe. 1993. Chromatin transitions during early *Xenopus* embryogenesis: changes in histone H4 acetylation and in linker histone type. *Dev. Biol.* 160:214–227.

Dimitrov, S., M.C. Dasso, and A.P. Wolffe. 1994. Remodeling sperm chromatin in *Xenopus laevis* egg extracts: the role of core histone phosphorylation and linker histone B4 in chromatin assembly. *J. Cell Biol.* 126:591–601.

Dworkin-Rastl, E., H. Kandolf, and R.C. Smith. 1994. The maternal histone H1 variant, H1M (B4 protein), is the predominant H1 histone in *Xenopus* pregastrula embryos. *Dev. Biol.* 161:425–439.

Earnshaw, W.C., B. Halligan, C.A. Cooke, M.M. Heck, and L.F. Liu. 1985. Topoisomerase II is a structural component of mitotic chromosome scaffolds. *J. Cell Biol.* 100:1706–1715.

Edwards, N.S., and A.W. Murray. 2005. Identification of *Xenopus* CENP-A and an associated centromeric DNA repeat. *Mol. Biol. Cell.* 16:1800–1810.

Fan, Y., T. Nikitina, E.M. Morin-Kensicki, J. Zhao, T.R. Magnuson, C.L. Woodcock, and A.I. Skoultchi. 2003. H1 linker histones are essential for mouse development and affect nucleosome spacing in vivo. *Mol. Cell. Biol.* 23:4559–4572.

Glynn, E.F., P.C. Megee, H.G. Yu, C. Mistrot, E. Unal, D.E. Koshland, J.L. DeRisi, and J.L. Gerton. 2004. Genome-wide mapping of the cohesin complex in the yeast *Saccharomyces cerevisiae*. *PLoS. Biol.* 2:10.1371/journal.pbio.0020259.

Haering, C.H., and K. Nasmyth. 2003. Building and breaking bridges between sister chromatids. *Bioessays.* 25:1178–1191.

Hagstrom, K.A., V.F. Holmes, N.R. Cozzarelli, and B.J. Meyer. 2002. *C. elegans* condensin promotes mitotic chromosome architecture, centromere organization, and sister chromatid segregation during mitosis and meiosis. *Genes Dev.* 16:729–742.

Hansen, J.C. 2002. Conformational dynamics of the chromatin fiber in solution: determinants, mechanisms, and functions. *Annu. Rev. Biophys. Biomol. Struct.* 31:361–392.

Harvey, A.C., and J.A. Downs. 2004. What functions do linker histones provide? *Mol. Microbiol.* 53:771–775.

Heck, M.M. 1997. Condensins, cohesins, and chromosome architecture: how to make and break a mitotic chromosome. *Cell.* 91:5–8.

Hudson, D.F., P. Vagnarelli, R. Gassmann, and W.C. Earnshaw. 2003. Condensin is required for nonhistone protein assembly and structural integrity of vertebrate mitotic chromosomes. *Dev. Cell.* 5:323–336.

Kapoor, T.M., T.U. Mayer, M.L. Coughlin, and T.J. Mitchison. 2000. Probing spindle assembly mechanisms with monastrol, a small molecule inhibitor of the mitotic kinesin, Eg5. *J. Cell Biol.* 150:975–988.

Kimura, K., and T. Hirano. 1997. ATP-dependent positive supercoiling of DNA by 13S condensin: a biochemical implication for chromosome condensation. *Cell.* 90:625–634.

Laloraya, S., V. Guacci, and D. Koshland. 2000. Chromosomal addresses of the cohesin component Mcd1p. *J. Cell Biol.* 151:1047–1056.

Losada, A., T. Yokochi, R. Kobayashi, and T. Hirano. 2000. Identification and characterization of SA/Scc3p subunits in the *Xenopus* and human cohesin complexes. *J. Cell Biol.* 150:405–416.

Maddox, P., A. Straight, P. Coughlin, T.J. Mitchison, and E.D. Salmon. 2003. Direct observation of microtubule dynamics at kinetochores in *Xenopus* extract spindles: implications for spindle mechanics. *J. Cell Biol.* 162:377–382.

Malik, H.S., D. Vermaak, and S. Henikoff. 2002. Recurrent evolution of DNA-binding motifs in the *Drosophila* centromeric histone. *Proc. Natl. Acad. Sci. USA.* 99:1449–1454.

Mao, Y., A. Abrieu, and D.W. Cleveland. 2003. Activating and silencing the mitotic checkpoint through CENP-E-dependent activation/inactivation of BubR1. *Cell.* 114:87–98.

Mayer, T.U., T.M. Kapoor, S.J. Haggarty, R.W. King, S.L. Schreiber, and T.J. Mitchison. 1999. Small molecule inhibitor of mitotic spindle bipolarity identified in a phenotype-based screen. *Science.* 286:971–974.

Murray, A.W. 1991. Cell cycle extracts. *Methods Cell Biol.* 36:581–605.

Ohsumi, K., C. Katagiri, and T. Kishimoto. 1993. Chromosome condensation in *Xenopus* mitotic extracts without histone H1. *Science.* 262:2033–2035.

Ono, T., A. Losada, M. Hirano, M.P. Myers, A.F. Neuwald, and T. Hirano. 2003. Differential contributions of condensin I and condensin II to mitotic chromosome architecture in vertebrate cells. *Cell.* 115:109–121.

Ono, T., Y. Fang, D.L. Spector, and T. Hirano. 2004. Spatial and temporal regulation of Condensins I and II in mitotic chromosome assembly in human cells. *Mol. Biol. Cell.* 15:3296–3308.

Poirier, M.G., and J.F. Marko. 2002. Mitotic chromosomes are chromatin networks without a mechanically contiguous protein scaffold. *Proc. Natl. Acad. Sci. USA.* 99:15393–15397.

Shen, X., L. Yu, J.W. Weir, and M.A. Gorovsky. 1995. Linker histones are not essential and affect chromatin condensation in vivo. *Cell.* 82:47–56.

Steffensen, S., P.A. Coelho, N. Cobbe, S. Vass, M. Costa, B. Hassan, S.N. Prokopenko, H. Bellen, M.M. Heck, and C.E. Sunkel. 2001. A role for *Drosophila* SMC4 in the resolution of sister chromatids in mitosis. *Curr. Biol.* 11:295–307.

Swedlow, J.R., and T. Hirano. 2003. The making of the mitotic chromosome: modern insights into classical questions. *Mol. Cell.* 11:557–569.

Thoma, F., and T. Koller. 1977. Influence of histone H1 on chromatin structure. *Cell.* 12:101–107.

Thoma, F., T. Koller, and A. Klug. 1979. Involvement of histone H1 in the organization of the nucleosome and of the salt-dependent superstructures of chromatin. *J. Cell Biol.* 83:403–427.

Tymowska, J. 1977. A comparative study of the karyotypes of eight *Xenopus* species and subspecies possessing a 36-chromosome complement. *Cytogenet. Cell Genet.* 18:165–182.

Van Hooser, A.A., I.I. Ouspenski, H.C. Gregson, D.A. Starr, T.J. Yen, M.L. Goldberg, K. Yokomori, W.C. Earnshaw, K.F. Sullivan, and B.R. Brinkley. 2001. Specification of kinetochore-forming chromatin by the histone H3 variant CENP-A. *J. Cell Sci.* 114:3529–3542.

Vernos, I., and E. Karsenti. 1996. Motors involved in spindle assembly and chromosome segregation. *Curr. Opin. Cell Biol.* 8:4–9.

Wignall, S.M., R. Deehan, T.J. Maresca, and R. Heald. 2003. The condensin complex is required for proper spindle assembly and chromosome segregation in *Xenopus* egg extracts. *J. Cell Biol.* 161:1041–1051.

Woodcock, C.L., and S. Dimitrov. 2001. Higher-order structure of chromatin and chromosomes. *Curr. Opin. Genet. Dev.* 11:130–135.